Experimental status of ^{7}Be production and destruction at astrophysical relevant energies

2016 J. Phys.: Conf. Ser. 665 012002

(http://iopscience.iop.org/1742-6596/665/1/012002)

Experimental status of ^{7}Be production and destruction at astrophysical relevant energies

A Di Leva[1,2], L Gialanella[3,2], F Strieder[4]

[1] Dipartimento di Fisica, Università di Napoli Federico II, Naples, Italy
[2] INFN Sezione di Napoli, Naples, Italy
[3] Dipartimento di Matematica e Fisica, Seconda Università di Napoli, Caserta, Italy
[4] Institut für Experimentalphysik, Ruhr-Universität Bochum, Bochum, Germany

E-mail: antonino.dileva@unina.it

Abstract. The production and destruction of ^{7}Be plays a significant role in the Big Bang Nucleosynthesis as well as in the framework of the solar neutrino. The ^{3}He$(\alpha,\gamma)^7$Be reaction cross sections has been measured several times in the last decades, but the precision achieved on reaction rate determinations at the relevant astrophysical energies is not yet satisfactory. The experimental status of this reaction will be critically reviewed, and the theoretical descriptions available will be discussed.

The production and destruction of ^{7}Be plays a significant role in the Big Bang Nucleosynthesis (BBN) as well as in the framework of the solar neutrino physics. The production of ^{7}Be proceeds essentially through the ^{3}He$(\alpha,\gamma)^7$Be reaction, while the main destruction channels in the Sun are ^{7}Be$(p,\gamma)^8$B and ^{7}Be$(e^-,\nu)^7$Li. On the contrary in BBN several other channels are present ^{7}Be$(n,p)^7$Li, , ^{7}Be$(n,\alpha)\alpha$, ^{7}Be$(d,p\alpha)\alpha$, ^{7}Be$(\alpha,\gamma)^{11}$C.

In this paper the experimental status of the ^{3}He$(\alpha,\gamma)^7$Be cross section is reviewed and among the available theoretical models the one that best describes simultaneously the larger number of the existing datasets is determined. This will be done using a statistically consistent analysis, avoiding an inflation of the errors and trying to use as much experimental information as possible. As regards the solar neutrino physics, for the ^{3}He$(\alpha,\gamma)^7$Be reaction the relevant energy range is 22 keV that is the energy of the Gamow peak at the Sun's central temperature of 15 MK. For BBN, considering that the Gamow peak has a width of $\sim$ 300 keV, the relevant energy range spans from $\sim$ 100 to $\sim$ 900 keV.

The S-factor of the ^{3}He$(\alpha,\gamma)^7$Be has been measured many times either by detecting the prompt γ-rays emitted in the reaction [1, 2, 3, 4, 5], or by detecting the γ-ray that follows the electron capture decay of ^{7}Be (*activation method*) [6, 7, 8, 9] and [10]. In some cases both methods were used concurrently: in [11], in [12, 13, 14] (the LUNA measurements), and in the work of Brown *et al.* [15]. Additionally the direct detection of the ^{7}Be nuclei produced in the reaction was exploited with the recoil separator ERNA [16], whereas activation and prompt γ-ray measurement were also performed. This measurement spans the largest energy range 0.65 to 3.15 MeV, and shows a significant discrepancy, on both the absolute scale and the energy dependence, with the results of [1], i.e. the data set with the largest energy range overlap. This questioned the fact that the simple picture of a pure external capture is not sufficient to describe this process. The results of ERNA have been recently confirmed by [9] and [10]. The results

of a new measurement [17] became available after the present analysis was completed, and are therefore not considered in the following.

An excellent agreement is found among the different datasets around $E_{\rm cm} = 1\,\mathrm{MeV}$, see figure 1. The comparison of data sets with overlapping energy range is straight forward, for the others the use of theoretical models is mandatory. The quantitative estimation on the agreement of the various experiments with each other needs a proper statistical analysis, taking into account the statistical and systematic uncertainty for each measurement.

Several models predicting the S-factor of the $^3\mathrm{He}(\alpha,\gamma)^7\mathrm{Be}$ are available in literature. Since the $^3\mathrm{He}(\alpha,\gamma)^7\mathrm{Be}$ is considered an external capture, the cross section is calculated from the electromagnetic operator expanded as electric and magnetic multipole operators, connecting the initial and final state wave functions. Depending on the way the wave functions are determined the models can be classified in two different groups: potential models and microscopic models. In the potential models the initial wave function is expressed as a function of the experimentally determined elastic scattering phase shifts. The final wave function depends on the reduced widths of the bound state, that can be derived from the measurement of $\sigma_{\gamma 429}/\sigma_{\gamma \mathrm{gs}}$. Thus the only free parameter in the model is normalisation constant that is obtained from a fit to the cross section data.
The microscopic models, instead, try to describe the 7 nucleon system, in a more or less detailed way, as clusters of nucleons interacting through a nucleon-nucleon (NN) potential. The parameters of the NN potential are adjusted to match the properties of target, projectile, and compound system, like scattering phase shifts and energy levels. The cross section calculated in this approach contains no absolute intensity parameter.

In the following the models given in [18, 19, 20, 21, 22, 23, 24] will be considered. Although the calculation of [23] is based on R-matrix, since no resonances are present in the energy range considered, it is similar to a potential model calculation, indeed very similar to the predictions of [25]. The models are usually claimed to be valid for $E_{\rm cm} \lesssim 2\,\mathrm{MeV}$, therefore comparison with data will be limited to this energy range.

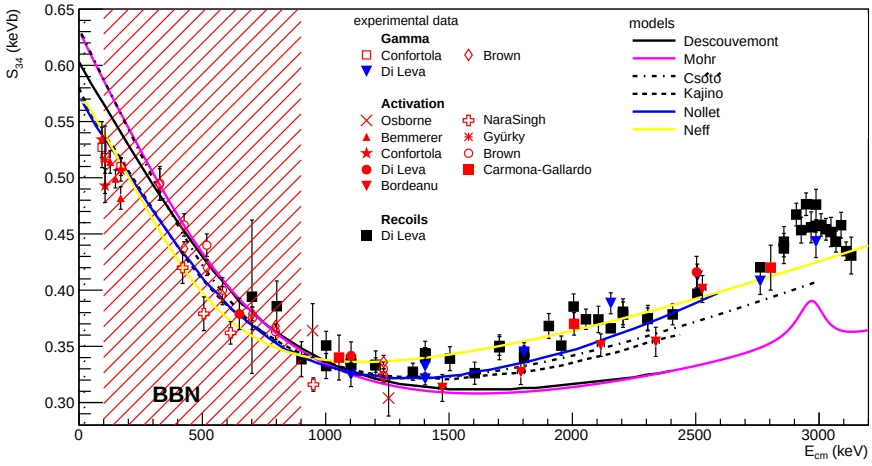

Figure 1. Comparison of the models with respect to experimental data. In this plot the curves are arbitrarily scaled in order to match the experimental data a $E_{\rm cm} \simeq 1\,\mathrm{MeV}$.

Unfortunately a global analysis of all the experimental data available is not possible, since in several works [1, 2, 3, 5] the quoted uncertainties include systematic errors, and a deconvolution of the errors is not possible on the basis of the published information. Thus the results obtained by least squares fits to these data sets would be not statistically correct. The works of [6, 4, 7]

measured each a single data point, so they provide no test of the model energy dependence, even though they may be used to estimate the absolute intensity. Anyhow the results of [7] are model dependent, and therefore will not be considered.
Hence to establish which calculation better describes the experimental data a least squares fit of each model is performed separately to: [11] prompt γ, [11] activation, [8], LUNA prompt γ [14], LUNA activation [12, 13, 14]), [15] prompt γ, [15] activation, ERNA recoil and activation [16], [9] and [10]. The fits of the model to the data are obtained by scaling each calculation by a constant factor c. This procedure is somewhat questionable for microscopic models, but the possible inaccuracy resulting from the scaling stays small if $c \approx 1$.
The minima of the least squares function L are given in table 1. If L follows a χ^2 probability

Table 1. Least square function minima, $\mathrm{LSF}_{\mathrm{min}}$, of the fits of the different models to the data sets in the energy range $E_{\mathrm{cm}} \leq 2.0\,\mathrm{MeV}$. The number of degree of freedom ν is indicated for each data set. The colours indicate different confidence level: fits with are marked green if $P(\chi^2 > \mathrm{LSF}_{\mathrm{min}}) > 5\%$ (good fit), yellow if $1\% < P(\chi^2 > \mathrm{LSF}_{\mathrm{min}}) < 5\%$, red if $P(\chi^2 > \mathrm{LSF}_{\mathrm{min}}) < 1\%$ (poor fit).

	[11] prompt	[11] activation	[8]	LUNA prompt	LUNA activation	[15] prompt	[15] activation	ERNA recoils	ERNA activation	[9]	[10]
ν	18	1	3	2	6	7	7	21	1	1	1
Descouvemont [23]	86	1.6	1.1	0.8	6.6	20	5.3	90	1.8	4.4	0.7
Kajino *et al.* [19]	83	2.3	1.4	0.7	6.6	9.6	12.3	38	0.4	1.4	0.2
Csoto [21]	95	2.5	0.9	1.4	6.7	19	3.4	25	1.1	0.5	0.1
Liu *et al.* [18]	79	2.4	2.8	0.1	7.3	17	21.5	41	0.3	1.1	0.3
Nollett [22]	83	2.5	0.9	0.7	6.6	11	10.0	23	0.7	0.3	0.02
Mohr [20]	91	1.5	2.0	1.2	6.6	31	6.6	93	2.7	4.5	0.7
Neff [24]	87	3.9	4.0	1.2	6.6	55	46	25	0.1	0.01	0.03

distribution its expectation value is the number of degrees of freedom ν. The fits are assumed consistent with the data considering a conservative confidence level of 99%, i.e. the probability that the model is discarded although it is correct is 1% or less.
The prompt γ-ray data of [11] are not fitted by any model, this is due to the fact that the external error is larger than the quoted internal error, therefore little information on the model can be obtained from this data set. The LUNA data sets are fitted equally well by all models. This is due to the fact that the energy range covered by the experiments is too narrow to give any information on energy behaviour of the S-factor. Although the data of [8], [9] and [10] cover a relatively wide energy interval they also do not constrain the model since they are well fitted by all calculations, because of the relatively low precision. Thus the only measurements that actually discriminate among available models are [15] and ERNA. The only models that are compatible with both data sets are [19] and [22], although one should be aware that the normalisation factor c is significantly different from 1 in both cases, ~ 1.15 and ~ 1.4, respectively. We could not quantify the uncertainty introduced by the normalisation.
It is worth noting that the recent microscopic calculation of [24] requires a normalisation close to 1, but it cannot describe sufficiently well the data of [15]. In fact the low energy points in [15] suggest a significantly steeper slope towards solar energies.

A quantitative analysis of the agreement between the different data sets is performed comparing the S-factor at zero energy $S_{34}(0)$ from the best fit of the models from [19] and [22], respectively. In figure 2 top panel the results according to the model of Kajino *et al.* [19] are shown. The total error σ_i affecting the extrapolation is obtained adding quadratically the systematic error of each individual measurement and the statistical error obtained by the fitting procedure. In those cases where two experimental techniques were used, the results are combined, taking into account the common systematic uncertainty according to the prescription of [26].
Although the measurements of [8] and [9] were carried out with the same experimental setup, if a common systematic uncertainty of 1% is assumed, the $S_{34}(0)$ values obtained in the present

Figure 2. Top panel: extrapolated $S_{34}(0)$ values according to the model of [19], the continuous line represents the weighted average of the compatible values, while the dashed lines the uncertainty. Very similar results are obtained with the model of [22]. Bottom panel: solid curve calculation of [22], dashed [19]. The curves are scaled to match the average value of $S_{34}(0)$ according to the model.

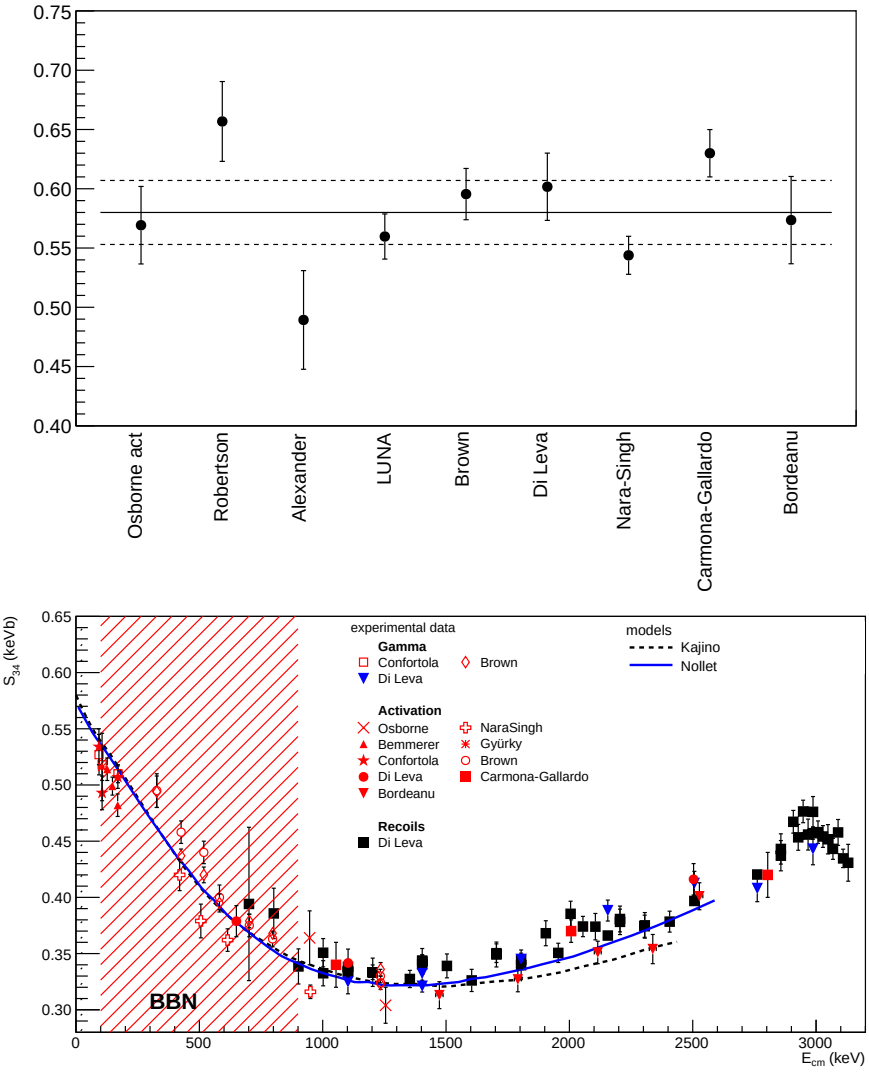

Table 2. Probability P of datasets to be compatible to each other, see text for details. The colours indicate different confidence level: $P \geq 32\%$ (agreement within 1σ) is highlighted in green, $5\% \leq P < 32\%$ (agreement within 2σ) is highlighted in yellow, $P < 5\%$ (no agreement) is highlighted in red. Top: extrapolation according to the [19] model. Bottom: extrapolation according to the [22] model.

	[6]	[4]	LUNA	[15]	ERNA	[8]	[9]	[10]
[11] activation	0.01	0.03	0.84	0.68	0.78	0.53	0.28	0.94
[6]		0.00	0.01	0.03	0.07	0.00	0.36	0.02
[4]			0.03	0.00	0.00	0.10	0.00	0.03
LUNA				0.26	0.42	0.64	0.15	0.77
[15]					0.93	0.27	0.59	0.73
ERNA						0.46	0.77	0.81
[8]							0.07	0.49
[9]								0.33

	[6]	[4]	LUNA	[15]	ERNA	[8]	[9]	[10]
[11] activation	0.01	0.02	0.82	0.71	0.82	0.51	0.42	0.86
[6]		0.00	0.00	0.02	0.04	0.00	0.11	0.01
[4]			0.02	0.00	0.00	0.08	0.00	0.05
LUNA				0.28	0.47	0.64	0.28	0.98
[15]					0.99	0.28	0.79	0.61
ERNA						0.49	0.87	0.75
[8]							0.12	0.68
[9]								0.36

analysis, with both the model of [22] or [19], are only marginally in agreement, therefore they are treated as completely independent experiments.
The obtained $S_{34i}(0)$ values, where i spans over the datasets, and relative uncertainty, are very similar for both calculations since their energy dependence differ significantly only for $E_{\rm cm} \gtrsim 1.5\,\mathrm{MeV}$, figure 2 bottom panel.

Given the model, the compatibility of the different $S_{34i}(0)$ values is evaluated with a Student's t-test with ν_i, ν_j degrees of freedom, for each pair i, j. In case $\nu = 1$ for one, or both, data sets the compatibility with zero of the difference is tested with a normal distribution with variance $(\sigma_i^2 + \sigma_j^2)$. The probability for the results to be compatible are reported in table 2.

The compatibility of the extrapolations is tested with a confidence limit of 95%. This test shows that the $S_{34}(0)$ extrapolated from the data of [6] and [4] are not statistically compatible with the determinations of some other experiments, and therefore are not used in averaging the values.

The best estimate for $S_{34}(0)$ is the weighted average of the results of the compatible experiments. The mean values for $S_{34}(0)$ are $0.579 \pm 0.027\,\mathrm{keV\,b}$ and $0.571 \pm 0.022\,\mathrm{keV\,b}$ for the [19] and [22] model, respectively. Since the internal error is smaller than the external error, the latter is quoted as the error on the mean value. Thus on the basis of this analysis the best estimate of

$$S_{34}(0) = 0.574 \pm 0.027\,\mathrm{keV\,b}$$

is suggested.

The quoted error represents the uncertainty to the determination of $S_{34}(0)$ due to statistical

fluctuations of the experimental information used. This analysis assumes that the energy dependence of the S-factor at energies below 1 MeV is correctly predicted by the [19] and [22] calculations. The contribution to the error that may come from the rather large normalisation of the models is difficult to evaluate. Recently the Solar Fusion II compilation [27] proposed a 0.02 keV b error, that has to be added to the statistical uncertainty quoted above, as a result of the uncertainty on the slope.

The result of the present analysis is similar to the one recommended by [27]. However it has to be stressed that the analysis described in this paper requires no inflation of the errors, thus preserving rigorously the probabilistic information of the uncertainty.

The authors thank F Terrasi for fruitful discussions about the manuscript.

[1] Parker P and Kavanagh R 1963 *Phys. Rev.* **131** 2578
[2] Nagatani K, Dwarakanath M and Ashery D 1969 *Nucl. Phys. A* **128** 325
[3] Kräwinkel H *et al.* 1982 *Z. Phys. A* **304** 307
[4] Alexander T *et al.* 1984 *Nucl. Phys.* **A427** 526
[5] Hilgemeier M *et al.* 1988 *Z. Phys.* **A329** 243
[6] Robertson R *et al.* 1983 *Phys. Rev.* **C27** 11
[7] Volk H *et al.* 1983 *Z. Phys.* **A310** 91
[8] NaraSingh B *et al.* 2004 *Phys. Rev. Lett.* **93** 262503
[9] Carmona-Gallardo M, Nara Singh B S, Borge M J G *et al.* 2012 *Phys. Rev. C* **86** 032801
[10] Bordeanu C, Gyürky G, Halász Z, Szücs T, Kiss G, Elekes Z, Farkas J, Fülöp Z and Somorjai E 2013 *Nucl. Phys. A* **908** 1 – 11 ISSN 0375-9474
[11] Osborne J *et al.* 1984 *Nucl. Phys.* **A419** 115
[12] Bemmerer D, Confortola F, Costantini H *et al.* 2006 *Phys. Rev. Lett.* **97** 122502 (pages 5)
[13] Gyürky G, Confortola F, Costantini H *et al.* 2007 *Phys. Rev. C* **75** 035805–+
[14] Confortola F, Bemmerer D, Costantini H *et al.* 2007 *Phys. Rev. C* **75** 065803–+ (*Preprint* `arXiv:0705.2151`)
[15] Brown T A D, Bordeanu C, Snover K A, Storm D W, Melconian D, Sallaska A L, Sjue S K L and Triambak S 2007 *Phys. Rev. C* **76** 055801–+ (*Preprint* `arXiv:0710.1279`)
[16] Di Leva A, Gialanella L, Kunz R, Rogalla D, Schürmann D, Strieder F, De Cesare M, De Cesare N, D'Onofrio A, Fülöp Z, Gyürky G, Imbriani G, Mangano G, Ordine A, Roca V, Rolfs C, Romano M, Somorjai E and Terrasi F 2009 *Phys. Rev. Lett.* **102** 232502 (pages 4) erratum: [Phys. Rev. Lett. 103, 159903 (2009)]
[17] Kontos A, Uberseder E, deBoer R, Görres J, Akers C, Best A, Couder M and Wiescher M 2013 *Phys. Rev. C* **87**(6) 065804
[18] Liu Q, Kanada H and Tang Y 1981 *Phys. Rev. C* **23** 645
[19] Kajino T, Austin S M and Toki H 1987 *ApJ* **319** 531–540
[20] Mohr P, Abele H, Zwiebel R, Staudt G, Krauss H, Oberhummer H, Denker A, Hammer J and Wolf G 1993 *Phys. Rev. C* **48** 1420–1427
[21] Csótó A and Langanke K 2000 *Few-Body Systems* **29** 121–130 (*Preprint* `arXiv:nucl-th/9906053`)
[22] Nollett K M 2001 *Phys. Rev. C* **63** 054002–+ (*Preprint* `arXiv:nucl-th/0102022`)
[23] Descouvemont P, Adahchour A, Angulo C, Coc A and Vangioni-Flam E 2004 *ADNDT* **88** 203–236
[24] Neff T 2011 *Phys. Rev. Lett.* **106**(4) 042502
[25] Tombrello T and Parker P 1963 *Phys. Rev.* **131** 2582
[26] D'Agostini G 1994 *Nucl. Instr. Meth. A* **346** 306–311
[27] Adelberger E G *et al.* 2011 *Rev. Mod. Phys.* **83**(1) 195–245